



A six-circle diffractometer with atmosphere- and temperature-controlled sample stage and area and line detectors for use in the G2 experimental station at CHESS

D. E. Nowak¹, D. R. Blasini², A. Vodnick¹, B. Blank^{3,4}, M. W. Tate⁵, A. Deyhim³, D.-M. Smilgies⁶, H. Abruña², S. M. Gruner^{5,6}, and S. P. Baker¹

1. Cornell University, Department of Materials Science and Engineering, Ithaca, NY 14853

2. Cornell University, Department of Chemistry and Chemical Biology, Ithaca, NY 14853

3. Advanced Design Consulting USA, Inc., Lansing NY, 14882

4. SpaceMill Sciences Corp., Freeville, NY 13068

5. Cornell University, Department of Physics, Ithaca, NY 14853

6. Cornell High Energy Synchrotron Source, Wilson Laboratory, Ithaca, NY 14853

ABSTRACT

A new diffractometer system was designed and built for the G2 experimental station at the Cornell High Energy Synchrotron Source (CHESS). A six-circle κ -goniometer, which provides better access to reciprocal space compared to Eulerian cradles, was chosen primarily to perform large angle Bragg diffraction on samples with preferred crystallographic orientations, and can access both horizontal and vertical diffraction planes. A new atmosphere- and temperature-controlled sample stage was designed for thin film thermomechanical experiments. The stage can be operated in ultra-high vacuum and uses a Be dome x-ray window to provide access to all scattering vectors above a sample's horizon. A novel design minimizes sample displacements during thermal cycling to less than 160 μm over 900°C and the stage is motorized for easy height adjustments, which can be used to compensate for displacements from thermal expansion. A new area detector was built and a new line detector was purchased. Both detectors cover a large region in reciprocal space providing the ability to measure time resolved phenomena. A detailed description of the design and technical characteristics are given. Some capabilities of the diffractometer system are illustrated by a strain analysis on a thin metal film and characterization of organic thin films with grazing-incidence diffraction. The G2 experimental station, as part of CHESS, is a national user facility and is available to external users by application.

1. INTRODUCTION

A very flexible general-purpose diffractometer system has been added to the G2 experimental station at the Cornell High Energy Synchrotron Source (CHESS). The G2 station is a shared user facility supported by the National Science Foundation. The new diffractometer system was designed around thin film thermomechanical experiments using x-ray diffraction strain analysis methods [1-4], and surface sensitive scattering experiments using Grazing Incidence - Reciprocal

Space Mapping (GI-RSM) [5]. The instrument can easily be adapted to work with a wide range of experimental setups. The new system features a six-circle κ -diffractometer, an atmosphere- and temperature-controlled sample stage, an area detector, and a line detector.

A six-circle κ -diffractometer design was chosen because it best meets all of the requirements of both the thermomechanical and GI-RSM experiments. For the thermomechanical experiments, strains are determined from shifts in Bragg peaks that are typically measured at large Bragg angles. Large Bragg angles are used to increase strain resolution by minimizing errors caused by a misalignment of a sample or the incident x-ray beam. Because thin films typically have grains with preferred crystallographic orientations relative to the film surface, sample rotations are constrained. For these reasons, a κ -goniometer was selected instead of the more traditional Eulerian cradle goniometer, which obstructs some high angle Bragg peaks. A split-ring Eulerian cradle does not obstruct large angle Bragg peaks, but the break in the ring adds compliance, especially in the vertical diffraction geometry, that would increase measurement errors and decrease strain resolution.

Because a shift in Bragg peak is used to determine strains, a high resolution in Bragg angle is necessary. Therefore, the thermomechanical experiments are performed using the vertical diffraction geometry because vertical beam collimation is better than horizontal beam collimation at synchrotron sources. In contrast, the horizontal scattering geometry was chosen for GI-RMS measurements because the wider horizontal beam provides more photons for grazing incidence scattering geometries. The detector arm consists of a vertical rotation stage attached to a horizontal rotations stage and accommodates both types of experiments using the same instrument. The detector arm motion covers more than an octant of scattering angles, which is beneficial if sample rotations are constrained. In particular, a large region in reciprocal space is available for the GI-RSM experiments.

The new sample stage was designed primarily for the thin film thermomechanical strain measurements. Because thin films are usually adhered to a rigid substrate, the use of traditional mechanical testing techniques, such as uni-axial tensile testing, typically cannot be used. Instead, thermomechanical tests have been developed to measure thin film mechanical properties [6,7]. Thermomechanical tests use the difference in thermal expansion coefficients between a film and substrate to apply a strain in the film by a change in temperature. The new sample stage provides a method to controllably change the sample temperature (*i.e.* strain) in an oxygen free environment, which is particularly important in metal thin films that oxidize at elevated temperatures.

The new detectors provide a means to collect data quickly. During a thermomechanical experiment the temperature is changed incrementally and held while multiple Bragg diffraction peaks are measured. Stresses relax during the hold at constant temperature at a rate that depends on the absolute stress and temperature. Therefore, acquiring diffraction peaks quickly is necessary to capture the initial stress state and any time dependent relaxation behavior. Both the line detector and area detector are capable of capturing a complete diffraction peak simultaneously, which significantly decreases measurement time. These detectors are also obviously advantageous for the GI-RSM experiments, where typically small scattering intensities over large ranges in reciprocal space must be collected. Higher sample throughput is highly advantageous at synchrotron sources with limited beam time.

In this paper we describe the components of the new diffractometer system and present some of their technical characteristics. Some capabilities of the system are demonstrated in a discussion of thin film thermomechanical measurements of a bicrystal (011) Al film on a Si

substrate and GI-RSM experiments on a 10 layer octodecyl phenol Langmuir-Blodgett (LB) film on a Si substrate.

2. DESCRIPTION

The new diffractometer system was designed to work in the G2 experimental station. The G2 station uses an “x-ray transparent” Be (0002) monochromator/beam splitter to share an intense x-ray beam from a multi-layer monochromator with the G3 experimental station. A range of incident beam energies between 8 and 16 keV are accessible. The Be crystal is used as a single side bounce monochromator operating in Laue transmission mode and diffracts a 0.1% energy bandpass of the beam from the multilayer mirror into the G2 station. The remaining beam that is not diffracted into the G2 station continues into the G3 station through a lead enclosed beam pipe.

2.1. DIFFRACTOMETER

A schematic representation of the diffractometer is shown in Fig. 1. The diffractometer, designed and fabricated in collaboration with Advanced Design Consulting USA, Inc (Lansing, NY), consists of six rotation stages, four for sample alignment and two for detector alignment. The basic naming convention used by You [8] has been adopted here but has been adapted to include a κ -goniometer, which is comprised of the inner three sample rotation stages, $K\phi$, κ , and $K\eta$. The fourth sample rotation, μ , is used as the θ rotation in horizontal diffraction mode and is used to align the diffractometer in vertical diffraction mode by making the $K\eta$ axis perpendicular to the incident x-ray beam. This alignment must be done when the beam energy is changed because by using the side bounce monochromator the beam direction changes with energy. The two detector rotation stages, ν and δ , are independent of the sample rotation stages. When operating in vertical or horizontal diffraction mode, the δ or ν rotation, respectively, is used as the 2θ rotation. Both detector rotations can be used simultaneously to increase the coverage of reciprocal space.

All six rotation stages are driven by stepper motors and use microstepping. Rotations are controlled through SPEC (Certified Scientific Software, 2005) software on a computer running a Linux operating system. SPEC provides a geometry code for six-circle diffractometers based on algorithms given by You [8] and includes the κ -goniometer configuration. For simplicity, all sample rotations are calculated in Eulerian geometry [9] using three orthogonal pseudo axes, η , χ , and ϕ . SPEC then translates the pseudo rotations into real motor positions based on the following set of equations [10]:

$$K\eta = \eta - \arcsin(-\tan(\chi/2)/\tan(\alpha)) \quad (1)$$

$$K\phi = \phi - \arcsin(-\tan(\chi/2)/\tan(\alpha)) \quad (2)$$

$$\kappa = 2\arcsin(\sin(\chi/2)/\sin(\alpha)) \quad (3)$$

where α is the angle between the $K\eta$ and κ axes and was specified to be 50° .

Material selection for the diffractometer design was influenced by two competing factors, a relatively large load from sample stages and the physical size of the G2 experimental station. The sample stage, details given below, has a stainless steel construction designed for Ultra High Vacuum (UHV) sample environments and weighs approximately 8 kg. With this load, high stiffness diffractometer components are required to prevent sample displacements from the center of rotation of the diffractometer. A target tolerance of $50\ \mu\text{m}$ was established. Greater stiffness can be achieved with larger rotation stages and stiffer materials. Although a steel

construction would provide greater stiffness, it would also increase the total weight of the diffractometer and require even larger rotation stages. The physical size of the G2 experimental station creates an upper limit on the size of the diffractometer and therefore the size of the rotation stages and materials used for construction. All six rotation stages of varying sizes were manufactured by Huber Diffraktionstechnik GmbH & Co. KG (Rimsting, Germany) using aluminum alloy housings and provide excellent stiffness to weight ratios. Larger support structures were produced from cast aluminum alloy by Elmira Pattern and Foundry Co. (Elmira, NY) and smaller structures were machined from aluminum alloy plate stock.

To reduce sample displacements arising from elastic deflections of the diffractometer all rotation stages are counterbalanced with lead weights. The counterbalances put the center of gravity of the load on each rotation stage as close as possible to the center of the rotation bearings. Because loads on the three inner stages change significantly for different rotations the counterbalances were designed to minimize the motion of the location of the center of gravity of the load on each rotation over the range of possible rotations.

The diffractometer was designed to be easy to setup and compatible with existing equipment. A working distance (the distance between the $K\phi$ interface plate and the center of rotation) of 129 mm was incorporated into the design to be consistent with other diffractometers at CHESS. Different detector assemblies are accommodated by using an easy to modify X48 precision rail system from Newport (Irvine, CA). The diffractometer is bolted to a motorized table that provides a convenient method to align the diffractometer with the incident x-ray beam. A 3-point kinematic mount is used to position the table height, pitch and roll. The diffractometer sits on top of horizontal Thompson rails and can be moved with a motorized lead screw to follow the x-ray beam when the energy is changed.

2.2. Sample Stage

A schematic representation of the sample stage, designed and fabricated in collaboration with Advanced Design Consulting USA, Inc (Lansing, NY), is shown in Fig. 2, where a cross-sectional view of the sample stage mounted on a rotation stage and a detailed view of the heater assembly are presented. A novel system was designed to minimize thermal expansion in a direction normal to the film surface (z -direction) that also maintains a clear path for incident and diffracted x-ray beams. To prevent obstructions to the x-ray path from the assembly, the heater and a glass ceramic (Macor®) insulator were recessed into a copper support using thin positioning lips at the top surface of the heater and insulator. The positioning lips for the heater and insulator are 0.125 cm and 0.250 cm in thickness, respectively, which produces a minimal thermal displacement of 33 μm in the z -direction over the total temperature range of the heater, room temperature to 900°C. The Cu support is water-cooled to minimize thermal displacements and provides a thermal conduction path when cooling a sample. Samples are held against the heater with clips that can be placed in different positions to avoid interference with the x-ray beams and are thermally isolated from the Cu support by glass ceramic spacers. The heating element was custom built by HeatWave Labs (Watsonville, CA), it is 3.18 cm in diameter and is constructed from a molybdenum shell with an alumina potting.

The heater assembly sits on a glass ceramic ball bearing on top of the vertical sample drive and is held in place by four adjustable screws. This attachment can be used like a two axis goniometer and allows the heater assembly to be adjusted to bring the sample normal parallel to the diffractometer $K\phi$ rotation axis. Translation in the z -direction is motorized and consists of a finely threaded rod with precision slides that maintain alignment. The translation is driven by a

stepper motor that is also controlled with the diffractometer software, SPEC. The threaded rod and slides are separated from the sample environment by a vacuum bellows.

The sample environment is enclosed within a stainless steel box measuring 8.59 cm per side with 6 conflat flange ports. The heater assembly puts the sample surface above the top flange and is capped with a beryllium dome (Brush Wellman, Inc., Fremont, CA) that was brazed to a conflat flange. The dome has a 5.08 cm diameter and allows all reflection geometries to be used during experiments. Sample exchange requires removing the dome to access the sample. A copper cooling tube is clamped to the conflat flange that is brazed to the beryllium dome to remove heat from the beryllium during a thermal cycle. The four ports around the sides of the cube provide freedthroughs to give access for thermocouples, electrical power to the heater, cooling water and atmospheric controls. Four thermocouples are used to monitor the thermal profile of the heater, sample, insulator and water-cooled Cu support. Thermocouple temperature readings are measured with a digital multimeter and TCSCAN card (Keithley Instruments, Inc., Cleveland, OH). Power to the heater is controlled by a PID controller (Eurotherm, Inc., Leesburg, VA). A LabView (National Instruments, Austin, TX) program was written in-house to remotely control and record temperatures. Cooling water for both the water-cooled Cu support and the beryllium dome are supplied by a re-circulating chiller (Julabo USA, Inc., Allentown, PA). The flow rate through the water-cooled Cu support is 2.5 l/h. The sample atmosphere can be either a constant flow of forming gas (such as 900 ppm CO with balance N₂) or evacuated through a vacuum hose by turbo molecular and rotary vane pumps (Pfeiffer Vacuum, Nashua, NH). The sample stage can be bolted directly to the $K\phi$ rotation stage using a modified interface plate.

2.3 Detectors

Two new detectors were added to the G2 instrumentation, one area detector and one line detector. The area detector was built in-house based on a fiber-optic/charged-coupled-device (CCD) design [11], a schematic representation of the detector is shown in Fig. 3. The detector works by converting x-rays to visible light using a phosphor screen. A fiber-optic taper is used to de-magnify the image produced on the phosphor screen and transmit it to a CCD where it is converted to a digital image. The primary component of this detector is a scientific-grade CCD, model KAF-1001E Blue-Plus from Eastman Kodak Company (Rochester, NY). The Blue-Plus CCD was selected because it has a very high quantum efficiency for shorter wavelengths of light. In traditional CCDs, blue light is absorbed in the polysilicon electrodes on top of the light-sensitive silicon volume. This can be overcome by using thinned, back-illuminated CCDs, but these CCDs are delicate and expensive. The Blue-Plus CCD uses indium tin-oxide electrodes to reduce absorption of blue light, resulting in a high quantum efficiency with front-side illumination. The CCD has 1024x1024 pixels with a pixel size of 24 μm . The CCD is optical-epoxy bonded to a fiber-optic taper (Incom, Inc., Charlton, MA) that has a 2.9:1 demagnification ratio, which gives a pixel size at the input face of the fiber-optic of 69.8 microns. A CCD controller (Finger Lakes Instrumentation LLC, IMG-series, Lima, NY) was integrated with a cryostat made to hold the fiber-optic/CCD assembly. A Gadolinium Oxysulfide:Tb (P-43) screen (Grant Scientific, Gilbert, SC) made of phosphor powder settled onto aluminized mylar at a density of about 15 mg/cm² was used. The phosphor screen is pressed against the fiber optic taper face by vacuum capture between the face and an opaque plastic/aluminum composite film.

An 1100X linear position sensitive detector (PSD) was purchased from Ordela, Inc. (Oak Ridge, TN). The 1100X uses the delay line technique [12] to determine the location of an

ionizing event along a wire anode 10 cm in length with an accuracy of 150 μm . Ionization occurs when a photon interacts with the XeCH_4 counting gas in the detector. Voltage pulses generated by the ionization event are pre-amplified and sent to a time-to-amplitude converter (Ordela, Inc, AIM-206). The pulse height signal is recorded by a multi-channel analyzer (MCA) that bins each ionization event into one of 1024 channels corresponding to its position along the counting wire. The MCA is an Ortec (Oak Ridge, TN) TRUMP-PCI-2k PCI board in the station computer and communicates directly with the data acquisition program, SPEC (Certified Scientific Software, 2005). For handling and displaying the MCA data, the macro package MCA.MAC from the European Synchrotron Radiation Facility (ESRF) was used. For data analysis, each channel from the MCA is converted to an angle in 2θ based on a calibration of the PSD. Bias for the PSD is supplied by a 0-3 kV adjustable high voltage power supply, model NHQ103M from FAST ComTec GmbH (Oberhaching, Germany).

3. TECHNICAL CHARACTERISTICS

3.1. Diffractometer

The six rotation axes were aligned to each other by a method described elsewhere [13]. The quality of the alignment was determined by measuring the sphere of confusion (SOC) and the angular deviation from parallelism or orthogonality for specific pairs of axes, given in Table 1. The SOC was measured using a tooling ball attached to the $K\phi$ rotation stage and placed at the center of rotation (COR) of the diffractometer along with a dial indicator attached to the detector arm. The maximum deviation recorded by the dial indicator for all rotations about all six axes is less than 150 μm . However, rotations about the δ axis contribute the largest displacements because of compliance in the detector arm. With δ fixed, the maximum deviation for all rotations about the other five axes is less than 30 μm . Angular deviations were measured with a granite machinist's cube and the dial indicator. Deviations for all pairs of axes were less than 100 μrad . The tooling ball is 44 mm in diameter, has a roughness less than 1 μm , is made of SiC and was purchased from Spheric-Trafalgar Ltd. (West Sussex, England). The granite cube is 7.62 cm per side, and has an accuracy of 0.1 μm . The digital read-out dial indicator has a precision of 1 μm and was purchased from Starrett (Athol, MA), model 2720-0.

The transformation between Eulerian-space and κ -space depends on the angle, α , between the $K\eta$ and κ axes. Because of machining tolerances, the design angle of 50° cannot be guaranteed. Therefore, the angle between the axes was measured directly. One simple method that can be used to measure the angle is based on Equation 3, re-written here in terms of α :

$$\alpha = \frac{\sin(\chi/2)}{\sin(\kappa/2)}. \quad (4)$$

Here we see that α can be calculated by measuring the rotation about the κ axis for a known χ rotation. First, the granite cube and dial indicator were used to set the 0° position for κ (and χ), which is defined as $K\phi$ collinear to $K\eta$. Then, the cube and indicator were used to find the rotation for κ such that $K\phi$ is orthogonal to $K\eta$, which is defined as χ equals 90° [9]. Such a rotation in κ was found at 135.325° , which corresponds to an α angle of 49.860° .

3.2. Sample Stage

The thermal characteristics of the sample stage were determined over a temperature cycle up to 900°C . Sample displacements caused by thermal expansion of the heater components were directly measured using x-rays. Measurements were performed using a rotating anode source and

a point detector (Bicron®, Saint-Gobain, Newbury, OH) focused on the direct x-ray beam. The beam was well collimated with two sets of incident beam slits and two sets of detector slits. A sample was placed at the center of the x-ray beam, which is found by scanning the sample through the beam and finding the position at which half of the intensity at the detector is blocked by the sample. These scans were repeated at 100°C intervals up to 900°C. The change in position as a function of temperature is shown in Fig. 4, top panel. Sample displacements over the thermal cycle are non-linear with temperature and have a maximum displacement of 155 μm. Using this calibration, errors in the sample height due to thermal expansion can be actively corrected using the vertical sample drive during an experiment. The sample drive has a precision of better than 2 μm, as measured with a dial indicator.

The source of the thermal displacements can be easily identified by consulting the thermal profile of the heater components, Fig. 4, bottom panel. The temperature at the sample, insulator and water-cooled Cu support are given as a function of the temperature of the thermocouple bonded to the underside of the heating element, which was used as the feedback sensor for the PID controller. The sample temperature maintains a nearly 1:1 ratio with the heating element and the insulator provides a good thermal barrier to the water-cooled Cu support but still allows the support to reach 125°C when the sample is at 900°C. This change in temperature of the Cu support contributes significantly to the total sample displacement in the z -direction because of thermal expansion. The non-linear behavior observed in the sample displacements can also be seen in the insulator and Cu support temperature profile. The cooling water temperature was maintained at $16^{\circ}\text{C} \pm 2^{\circ}\text{C}$ over the entire thermal cycle. The beryllium dome temperature was also monitored and did not exceed 70°C over the thermal cycle.

3.3. Detectors

The CCD detector was fully characterized using procedures described by Barna *et al.* [14]. The detector has a sensitivity of 17 electrons/x-ray at 8keV with a read noise of 11 electrons. The read time is 4 seconds. The dark current was 0.08 electrons/pixel/sec at the operating temperature of -40°C .

4. EXAMPLE APPLICATIONS

In this section, some capabilities of the new diffractometer system are presented using a strain analysis of a 1 μm bicrystal (011) Al film and reciprocal space mapping of a Langmuir-Blodgett (LB) film for examples.

4.1. Thin film thermomechanical testing

The new diffractometer system facilitates high precision thermomechanical testing of textured thin films where stresses are determined using x-ray diffraction strain analysis methods at different temperatures. The strain analysis methods are typically based on the $\sin^2(\psi)$ technique using the ψ -geometry [15,16]. In general, plane spacings, d , are measured at several different ψ angles, where ψ is the angle between the sample normal and the normal to the measured lattice planes. For certain stress states, crystal elasticity theory predicts that d will vary linearly with $\sin^2(\psi)$. By fitting a straight line to d vs. $\sin^2(\psi)$ data, the spacing of planes whose normals lie in the surface plane can be determined. With knowledge of the unstrained lattice parameter and elastic constants, the stress in the plane of the sample surface can be determined. For the six-circle κ -diffractometer, three sample rotations (η , χ , ϕ) and one detector rotation (δ) are used for

strain analysis. The incident and exit beam angles are equal such that $\eta = \delta/2$, the sample normal is collinear with ϕ , and $\chi = 90^\circ - \psi$.

An example strain analysis using the G2 diffractometer system was performed on a 1 μm bicrystal (011) Al film. The film was heteroepitaxially deposited on a single crystal (001) Si substrate by thermal evaporation following the method given in reference [17]. Films deposited by this method have only two orientation variants, OR1: $(011)_{\text{Al}} [100]_{\text{Al}} // (001)_{\text{Si}} [110]_{\text{Si}}$ and OR2: $(011)_{\text{Al}} [01\bar{1}]_{\text{Al}} // (001)_{\text{Si}} [110]_{\text{Si}}$. Both orientations have (011) planes parallel to the film plane and are rotated by 90° to each other in the plane of the film. The microstructure is characterized by columnar, interlocking grains that form a mazed grain structure with no triple junctions. Following the method given by Nowak, Thomas, and Baker [4], stresses in the plane of the film were determined in two orthogonal crystallographic directions, $[100]$ and $[01\bar{1}]$. The spacing between lattice planes of three sets of planes in the $[100]$ zone axis of OR2 and four planes in the $[01\bar{1}]$ zone axis of OR1 were measured using Bragg diffraction. Measured plane spacings and corresponding ψ and 2θ angles (the wavelength of the incident x-ray beam was 0.1457 nm) are given in Table 2. The Bragg peaks for most of these planes would not have been accessible using an Eulerian cradle. Because the orientation variants are rotated by 90° , spacings for lattice planes in the $[100]$ and $[01\bar{1}]$ zone axes were measured in the same diffraction plane removing the necessity for a sample normal rotation that would be required in a single crystal. Lattice strains were calculated from the measured plane spacings and used to extrapolate strains in the $[011]$, $[100]$ and $[01\bar{1}]$ directions from linear fits to the two data sets, Fig. 5. Calculated strains are given in Table 3 along with stresses that were calculated using Hooke's law and single crystal elastic constants for Al [18]. With no corrections, film strains on the order of 1×10^{-3} can be easily measured. With a calibration of the δ rotation, the systematic errors caused by compliance in the detector arm can be identified and removed, improving the resolution.

4.2. Grazing Incidence – Reciprocal Space Mapping

Grazing incidence-reciprocal space maps (GI-RSM) can be used to characterize the structure of self-organized molecular films and supermolecular assemblies. GI-RSM methods were first developed to study molecular self-organization at an air-water interface [19] but have been recently extended to thin films of molecules absorbed on glass or on silicon substrates [5]. By using a grazing incidence scattering geometry, the x-ray penetration depth is reduced so that the incident x-ray beam is mainly confined to the organic film, which decreases diffuse scattering from the substrate. The experimental geometry is defined by four angles (α , β , ψ and ϕ) [20]. The angle between the incident beam and the sample surface, α , is set below the critical angle of the substrate. The exit angle, β , also called the out-of-plane scattering angle, is measured along the line detector. The in-plane scattering angle is defined as ψ (Note, that ψ is redefined here for the GI-RSM setup). Finally, ϕ is the sample azimuth rotation, which can be used to align the substrate with the incident x-ray beam in samples that have preferred in-plane orientation. The sample is seated on a motorized height stage that precisely aligns the sample to the incident x-ray beam. Two diffractometer sample rotations (ϕ , η) and both detector rotations (δ , ν) are used in the GI-RSM geometry. The incident angle, α , is set using the η rotation and the sample azimuth rotation, ϕ , is collinear with the $K\phi$ axis of the diffractometer. The in-plane scattering angle, ψ , is set with the ν rotation, while the out-of-plane scattering angle, β , is measured on the line

detector. The range of β can be augmented using the δ rotation of the detector arm. The other two diffractometer sample rotations, χ and μ , are fixed at 90° and 0° , respectively.

A reciprocal space map is generated by scanning the line detector combined with an aperture-matched Soller collimator in ν . The line detector records a range of β angles for each ν position and the entire scan is compiled into a reciprocal space map. An example map is given in Fig. 6 for a ten layer octodecyl phenol Langmuir-Blodgett (LB) film on a Si substrate. We are indebted to Oleg Konovalov, ESRF, for providing this calibration sample. The Langmuir-Blodgett technique allows a layer-by-layer deposition of amphiphilic molecules creating well-defined supramolecular assemblies. Octodecyl phenol molecules form double-layers (head-to-head, tail-to-tail) on Si substrates. The molecules stand upright on the surface, as is evidenced by the lateral structure of the first order Bragg rod, around 17.4 degrees in ψ . The intensity modulation along this Bragg rod is related to the large unit cell dimension perpendicular to the surface. The partial rings through the film Bragg peaks indicate the mosaic structure of the LB films caused by fluctuations at the film/substrate interface and the internal interfaces of the layers.

The bottom panel in Figure 6 shows a simulated result of an in-plane powder diffraction scan derived from the GI-RSM, where the intensity in β was integrated between 0° and 2° and plotted as a function of γ . It can be clearly seen that the nature of features a-d can only be interpreted from the full GI-RSM: features a and b are scattering rods from the film. On rod b, only one Bragg peak has enough intensity to contribute to the rod significantly due to the molecule form factor. Feature c is due to the mosaic structure associated with Bragg peak b. Finally d appears to be a structureless scattering rod from the substrate.

At the time of writing we have applied the GI-RSM method to a large variety of samples, ranging from single-crystalline samples of molecular crystallites [5] to self-organized monolayers on GaAs surfaces [21] to surfaces of device-grade films of electro-optical materials [22] and fuel cell catalysts [23]. Grazing-incidence scattering can be complemented with x-ray reflectivity and fluorescence methods [24] on the κ -diffractometer, to offer a full spectrum of x-ray thin film analysis methods.

5. SUMMARY AND CONCLUSIONS

A new diffractometer system for the G2 experimental station was designed, constructed, and commissioned. The new system consists of a versatile six-circle κ -diffractometer, an environmental- and temperature-controlled sample stage, an area detector, and a line detector. Key features of the new instrumentation include:

- Six-circle κ -diffractometer: access to all scattering vectors above a sample's horizon, access to both horizontal and vertical diffraction geometries, compatible with existing sample stages, easy to modify experimental setups, convenient line-up with incident x-ray beam
- Sample stage: minimum sample displacements from thermal expansion, can actively correct for height errors induced by thermal expansion using a motorized stage, a very low oxygen atmosphere using either ultra-high vacuum (UHV) or forming gas, and a temperature range up to 900°C
- Area detector: large coverage of reciprocal space, low noise, good readout speed
- Line detector: single photon counting for noise-free detection of low scattering signals, compatible with large illuminated sample area when used in combination with a Soller collimator, increases sample throughput by decreasing measurement time

Combining these features provides an excellent system for thin film thermomechanical strain experiments and grazing incidence-reciprocal space mapping experiments for the characterization of organic thin films. Additionally, these features can easily be adapted to work with a wide range of other experiments and experimental setups.

6. ACKNOWLEDGMENTS

Support for this project was provided by the National Science Foundation through an Instrumentation for Materials Research grant (DMR-0216881), by the Department of Energy (DE-FG02-02ER46001), and by Cornell University through the Cornell Center for Materials Research. This work is based upon research conducted at the Cornell High Energy Synchrotron Source (CHESS) which is supported by the National Science Foundation and the National Institutes of Health/National Institute of General Medical Sciences under award DMR-0225180. Significant contributions were made by Joel Brock, Brian Clasby, Aaron Fleet, Jerry Houghton, Ted Luddy, Alan Pauling, and Dave Waterman. The authors would also like to thank the entire staffs of CHESS, Advanced Design Consulting, Inc and SpaceMill Sciences Corp. The bicrystal (011) Al sample was provided by Daan-Hein Alsem (LBNL) and Eric Stach (Purdue University). The octadecyl phenol Langmuir-Blodgett film was provided by Oleg Konovalov (ESRF).

7. REFERENCES

1. M.A. Korhonen and C.A. Paszkiet, *Scripta Metall.*, **23** (8), 1449-1453 (1989).
2. B.M. Clemens and J.A. Bain, *Mater. Res. Bull.*, **17** (7), 46-51 (1992).
3. R.P. Vinci, E.M. Zielinski and J.C. Bravman, *Thin Solid Films*, **262** (1-2), 142-53 (1995).
4. D.E. Nowak, O. Thomas and S.P. Baker, unpublished, (2006).
5. D.M. Smilgies, D.R. Blasini, S. Hotta and H. Yanagi, *J Synchrotron Radiat.*, **12**, 807-811 (2005).
6. W.D. Nix, *Metall. Trans. A*, **20A** (11), 2217-45 (1989).
7. O. Kraft and C.A. Volkert, *Adv. Eng. Mater.*, **3** (3), 99-110 (2001).
8. H. You, *J. Appl. Crystallogr.*, **32** (4), 614-23 (1999).
9. W.R. Busing and H.A. Levy, *Acta Crystallogr.*, **22**, 457-64 (1967).
10. D.E. Sands, *Vectors and Tensors in Crystallography* (Addison-Wesley Publishing Company, Inc., London, 1982).
11. M.W. Tate, E.F. Eikenberry, S.L. Barna, M.E. Wall, J.L. Lowrance and S.M. Gruner, *J. Appl. Crystallogr.*, **28**, 196-205 (1995).
12. C.J. Borkowski and M.K. Kopp, *Rev. Sci. Instrum.*, **46** (8), 951-962 (1975).
13. D.E. Nowak, Ph.D. dissertation, Cornell University, 2006.
14. S.L. Barna, M.W. Tate, S.M. Gruner and E.F. Eikenberry, *Rev. Sci. Instrum.*, **70** (7), 2927-34 (1999).
15. I.C. Noyan and J.B. Cohen, *Residual Stress Measurement by Diffraction and Interpretation*, (Springer-Verlag, New York, 1987).
16. H. Behnken and V. Hauk, *Thin Solid Films*, **193-194** (Part 1), 333-341 (1990).
17. N. Thangaraj, K.H. Westmacott and U. Dahmen, *Appl. Phys. Lett.*, **61** (1), 37-9 (1992).
18. K.H. Hellwege and A.M. Hellwege, *Landolt-Bernstein Numerical data and functional relationships in science and technology Group III: crystal and solid state physics*, (Springer-Verlag, New York, 1966).
19. J. Als-Nielsen, D. Jacquemain, K. Kjaer, F. Leveiller, M. Lahav and L. Leiserowitz, *Phys. Rep.*, **246** (5), 251-313 (1994).
20. D.-M. Smilgies, *Rev. Sci. Instrum.*, **73** (4), 1706-10 (2002).
21. C. McGuinness, D.R. Blasini, D.-M. Smilgies and D.L. Allara, unpublished, (2006).
22. D.R. Blasini, D.-M. Smilgies, S. Flores-Torres, H.D. Abruña, J. Slinker, J. Rivnay and G.G. Malliaras, unpublished, (2006).
23. D.R. Blasini, Y. Liu, D.-M. Smilgies and H.D. Abruña, unpublished, (2006).
24. D.R. Blasini, S. Flores-Torres, D.-M. Smilgies and H.D. Abruña, *Langmuir*, **22** (5), 2082-2089 (2006).

8. TABLE CAPTIONS

Table 1. Pairs of diffractometer axes that are parallel or orthogonal.

Table 2. Lattice planes with corresponding ψ and 2θ angles for planes in the [100] and $[01\bar{1}]$ zone axes that were measured for the $\sin^2(\psi)$ strain analysis.

Table 3. Strains and stresses determined for the three normal directions in a 1 μm bicrystal (011) Al film. *The stress in the [011] direction is defined as zero in the method.

9. TABLES

Table I.

Parallel	Orthogonal
δ and $K\eta$ for $\nu = \mu$	δ and ν
μ and ν	$K\eta$ and μ
$K\eta$ and $K\phi$ for $\chi = 0^\circ$	$K\eta$ and $K\phi$ for $\chi = 90^\circ$

Table II

[100] Zone Axis			[01$\bar{1}$] Zone Axis		
Plane	ψ	2θ	Plane	ψ	2θ
(133)	13.26°	103.29°	(042)	18.43°	107.13°
(333)	35.26°	138.39°	(040)	45.0°	92.04°
(422)	54.74°	123.61°	(04 $\bar{2}$)	71.57°	107.13°
(511)	74.21°	138.39°			

Table III.

Direction	Strain (%)	Stress (MPa)
[011]	-0.145	0*
[100]	0.114	134
[01 $\bar{1}$]	0.161	171

10. FIGURE CAPTIONS

- Figure 1. Schematic representation of the six-circle κ -diffractometer.
- Figure 2. a) Schematic representation of the sample stage attached to the $K\phi$ rotation stage and b) detailed view of the heater assembly.
- Figure 3. Schematic representation of the area detector [11].
- Figure 4. Top panel: height calibration of the sample stage during a thermal cycle. Sample displacements were determined at each temperature by scanning the sample through an x-ray beam and using the position at half the maximum intensity. Bottom panel: temperature calibration of the sample stage during a thermal cycle. The thermocouple attached to the underside of the heating element was used as the control thermocouple. The gray line has a slope of 1.
- Figure 5. $\text{Sin}^2(\psi)$ strain analysis for a 1 μm bicrystal (011) Al film. Strains and stresses based on this analysis are given in Table III.
- Figure 6. Top panel: GI-RSM image from a 10 layer octadecyl phenol Langmuir-Blodgett (LB) film, ψ is the in-plane scattering angle and β is the out-of-plane scattering angle. Bottom panel: A simulated in-plane powder diffraction scan derived from the GI-RSM. The intensity in β was integrated between 0° and 2° and plotted as a function of ψ . See text for an additional explanation.

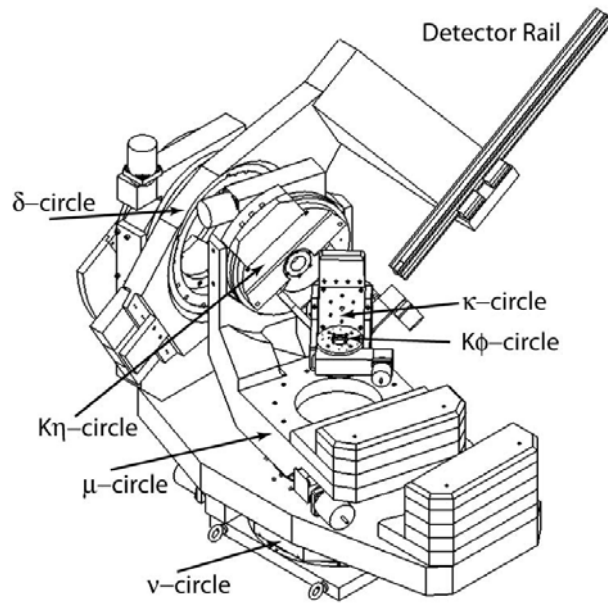


Figure 1

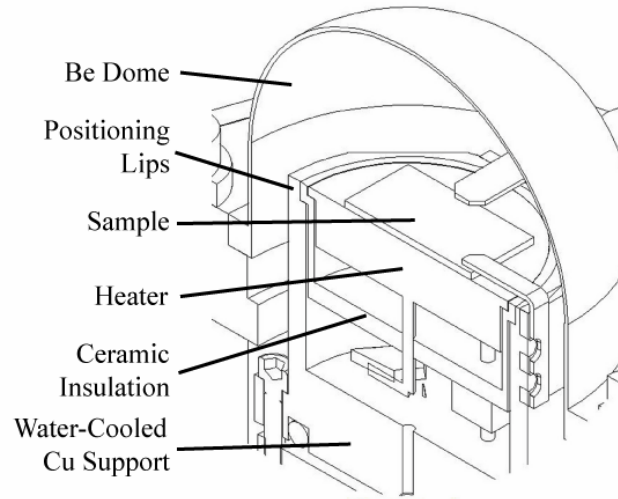
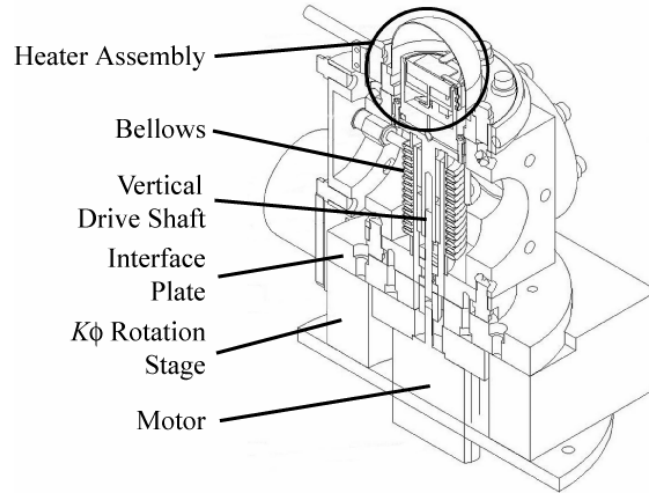


Figure 2

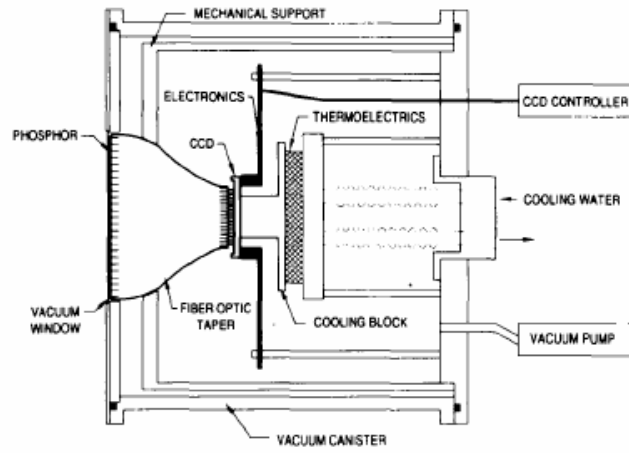


Figure 3

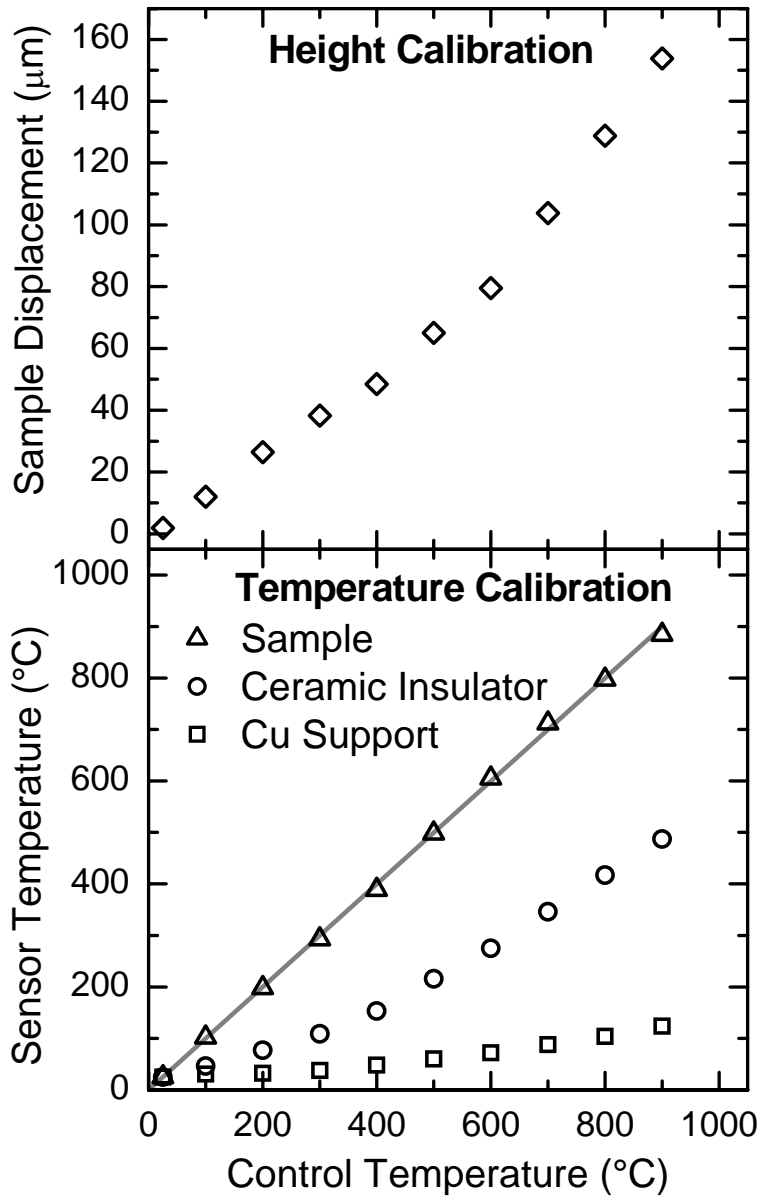


Figure 4

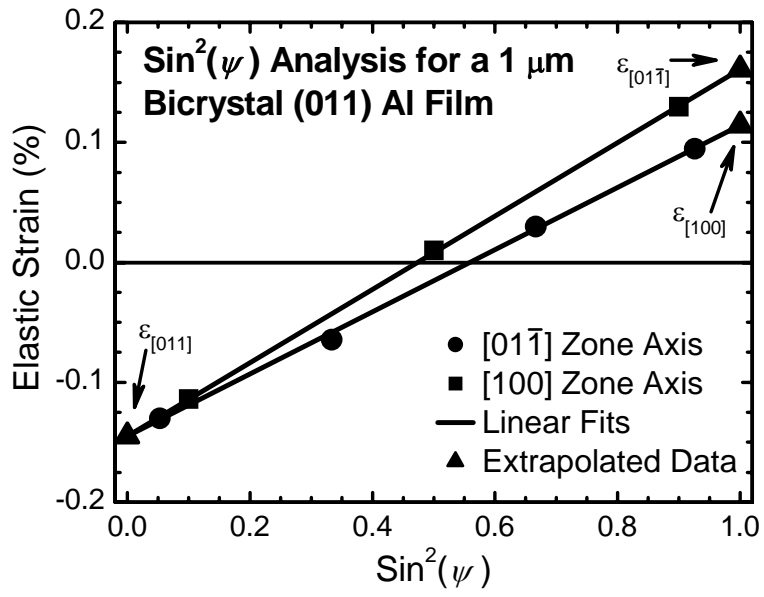


Figure 5.

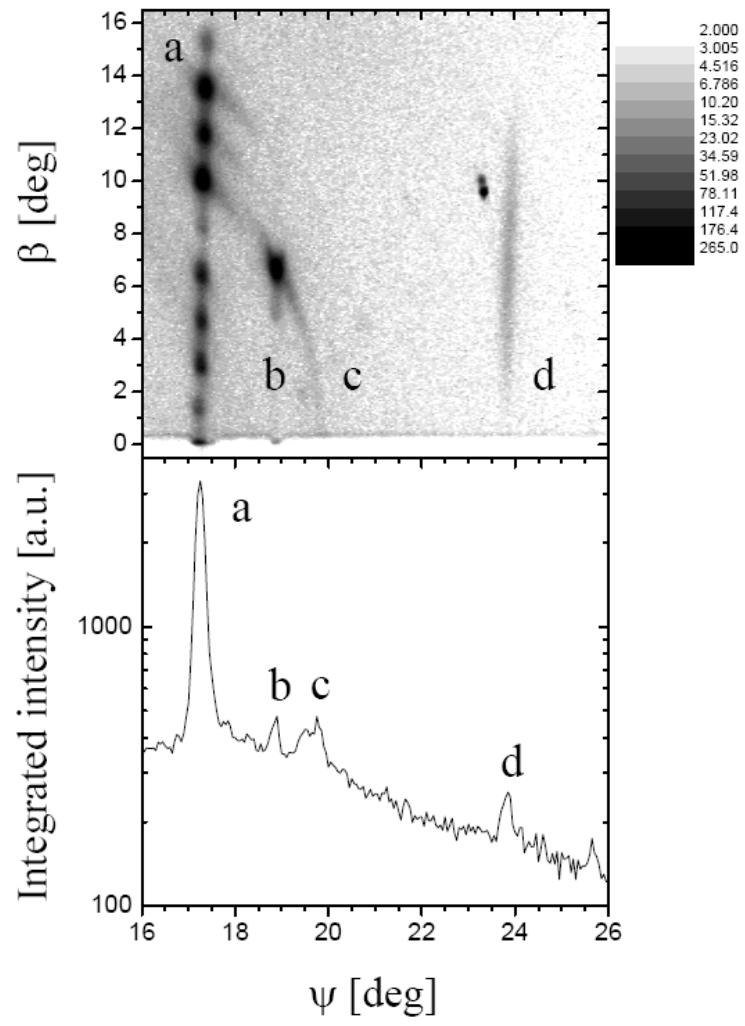


Figure 6.